

CHARACTERIZATION OF MEMBRANE OF POLY (L,CO-D,L-LACTIC ACID-CO-TRIMETHYLENE CARBONATE) (PLDLACO-TMC) (50/50) LOADED WITH SILK FIBROIN.

DOI:10.25177/JBE.2.1.1

ISSN: 2573-8100

AUTHOR: Marco Vinicius Chaud

Research

July 2017

Daniel Komatsu¹, Norberto Aranha², Marco Vinicius Chaud^{2*}, José Martins de Oliveira Júnior², Daniel Vinicius Mistura³; Adriana Motta¹; Eliana A. R. Duek^{1,3}

1. Laboratory of Biomaterials, Pontifical Catholic University of São Paulo - PUC-SP, Zip Code 18030095, Sorocaba, SP, Brazil.
2. Technological and Environmental Processes, University of Sorocaba- UNISO Zip-Code 18023-000 Sorocaba, SP, Brazil.
3. Faculty of Mechanical Engineering, University of Campinas, Zip Code 13083-860, Campinas, SP, Brazil.

CORRESPONDENCE AUTHOR

Marco Vinicius Chaud

Email: chaudmarco@gmail.com; Cell phone +55 15 981536692

CONFLICTS OF INTEREST

There are no conflicts of interest for any of the authors.

Received Date: 23th May 2017Accepted Date: 22th July 2017Published Date: 26th July 2017

Copy rights: © This is an Open access article distributed under the terms of Creative Commons Attribution 4.0 International License.

ABSTRACT

Silk produced by *Bombyx-mori* consists of two proteins sericin and fibroin. Silk Fibroin (SF) an attractive material for epithelial tissue regeneration. The aim of this study was to characterize membranes of PLDLACO-TMC:SF (2:1 w/w) once it could be used as a wound dressing to burn treatment and epithelial tissue regeneration. Membranes of Poly(L-co-D,L-lactic acid-co-TMC) with SF were prepared by casting method and it was analysed by: FTIR - there was no change in the PLDLA-co-TMC spectrum after SF has been added in polymers' solution, Swelling Test – the samples with SF had a different swelling behaviour of PLDLA-co-TMC. Membrane with SF showed swelling rate faster than PLDLA-co-TMC. Contact angle measurement - PLDLA-co-TMC (1:1 w/w) showed a contact angle value higher than samples with SF. SEM – the addition of SF in PLDLA-co-TMC apparently leaves the polymer surface more roughened. Tensile test - there was a decrease in the Young's modulus and there was an increase in the elongation at break of PLDLA-co-TMC:SF membrane, DSC – SF did not change the glass temperature (T_g) of PLDLAco-TMC. The membrane of PLDLA-co-TMC:SF was characterized and it has potential to be used as a wound dressing to burn treatment and epithelial tissue regeneration.

INTRODUCTION

Silk produced by *Bombyx-mori* consists of two proteins: sericin, which surrounds the fibers and fibroin which is the silk filament composed of highly organized regions with sheet-β crystals and semi crystalline, responsible for the elasticity of silk¹. The fibroin has several interesting properties such as compatibility with different types of mammalian cells, high permeability to oxygen and water vapor, biodegradability, minimal inflammatory response, antioxidant effect, these properties among others makes SF an attractive material for epithelial tissue regeneration. In addition, the fibroin also features high mechanical and microbial resistance, enabling their use as substrates for cell culture, enzyme immobilization, contact lenses, drug delivery agents and protection of wounds.¹⁻⁷ SF has been applied successfully performing as man-made blood-vessels⁸, surgical sutures and repair materials.⁹ Attachment of bioactive molecules to SF has many benefits to enhance the properties of bioactive molecules in solution for delivery both in vitro and in vivo, including the therapeutic efficacy in the body, thermal stability, storage stability, and lengthens the circulatory half-life and decreases immunogenicity and antigenicity.¹ In order to improve the performance of individual natural polymers, many blends have been developed, such as SF with calcium phosphate cements¹⁰ and blends of two or more degradable polymers¹¹; chitosan¹², hyaluronan¹³ and poly(vinyl alcohol)¹⁴ blends, amongst others, have been prepared using solution blending methods.

Among the degradable polymers stands out the copolymer poly (L,co-D,L-lactic acid) (PLDLA) that is widely used in the because of its good mechanical properties and biocompatibility. Though, the low elongation values of PLDLA make it susceptible to brittle fracture, which in turn limits its range of applicability.¹⁵ One of the ways to increase the elongation value of PLDLA is by inserting segments of trimethylene carbonate (TMC), an elastomeric aliphatic polycarbonate, alongside the PLDLA copolymer chain, to enhance the stability of the copolymer, giving rise to poly (L-co-D,L-lactic acid-co-TMC) (PLDLA-co-TMC).¹⁶ Therefore, an increase in the elongation value of PLDLA would be useful in expanding the applications of this material. An example of the possible applications for this material would be as wound dressing. In this work was obtained a composite membranes of poly (L-co-D,L-lactic acid-coTMC) (PLDLA-co-TMC) with lyophilized fibroin with potential to be used as wound dressing. The structural and mechanical aspects of the polymer samples with fibroin and the effect of sonication used for dispersion of fibroin were evaluated. Therefore the aim of this study is to characterize the membrane of PLDLA-co-TMC:SF (1:1 w/w) once it could be used as a wound dressing to burn treatment and epithelial tissue regeneration.

2. MATERIALS AND METHODS

2.1- Materials

L-lactide and D,L-lactide monomers were obtained from Purac Biochem (The Netherlands) and trimethylene carbonate (1,3 dioxan-2-one) (TMC) was obtained from Boehringer Ingelheim (Germany). The polymer, Poly (L,co-D,L-lactic acid-co-trimethylene carbonate) (PLDLA-co-TMC 1:1 w/w) was obtained as described by Motta & Duek, 2014.¹⁷

2.2- METHODS

2.1- Preparation of silk fibroin

Silk fibroin was obtained from cocoons of *bombyx mori* following a standard extraction protocol.¹⁸ LiBr (>99% purity, Sigma Aldrich, Germany) were used as such without further purification. Cocoons were cut into small pieces, boiled in 0.5 wt. % Na₂CO₃ solution at 98 °C for 1 hour to remove sericin from the silk fibers. After, the silk fibers were washed with deionized water several times and dried in oven at 50 °C for 24h. The silk fibers were dissolved in 1L of ternary solution CaCl₂ – Ethanol – Water (mole ratio 1:2:8) at 85 °C for 50 minutes. This solution was dialyzed for 3 days at room temperature in cellulose tubing with a molecular weight cut-off of 14,000 Dalton against deionized water replaced each 12 hours to remove CaCl₂ and others ions. The solution was centrifuged at 7,500 rpm. This solution was freezing at -80 °C for 24h and lyophilized to obtain fibroin in powders form.

2.2- Preparation of membranes

Membranes of PLDLA-co-TMC:SF (1:2 w/w) were prepared by the casting method. Initially the PLDLA-co-TMC was dissolved in chloroform (10% w/v) for 4h. After complete dissolution of PLDLA-co-TMC the SF (5%) was added and the mixture was kept under stirring (5 min) with probe-type ultrasonic homogenizer with two different potencies (50W or 100W) to improve the fibroin dispersion in the polymer solution. The adequate time to homogenize SF in the polymer solution was previously determined, and it was realized without cooling system. The samples exposed to 50W or 100W potency and called 50W (PLDLA-co-TMC/SF 1:2 w/w) and 100W ((PLDLA-co-TMC/SF 1:2 w/w).

After 5 min of sonication the PLDLA-co-TMC/SF solution was poured on a glass plate and this assembly was placed inside a glass box saturated with chloroform for 12 hours. Finally, the PLDLA-co-TMC/SF membranes were dried at room temperature.

2.3- Fourier Transform Infrared (FTIR) spectroscopy

FTIR spectra were recorded by the Perkin Elmer *Spectrum 65* Fourier transform infrared (FTIR) spectrometer with an ATR cell. Spectra over 4000-500 cm⁻¹ range were obtained by the co-addition of 64 scan with a resolution of 4 cm⁻¹.

2.4- Swelling test

Swelling tests were conducted under identical conditions for all the membranes. The bath temperature and maximum immersion time considered in this study was equal 37°C and 400h, respectively. For the phosphate buffer solution (pH 7.4) absorption measurements, the specimens were withdrawn from the phosphate buffer solution, wiped dry to remove the surface moisture, and then weighed using an electronic balance accurate to 10⁻⁴ g to monitor the mass change during the water absorption. The weight variation (weight %) absorbed by each sample was calculated from its initial weight (w_0) and its weight after absorption (w_t) as follows equation 1:

$$\text{Weight (\%)} = \left(\frac{W_t - W_0}{W_0} \right) \times 100 \quad \text{Eq. (1)}$$

2.5- Contact angle measurement

The wettability of the surfaces was evaluated by measuring the static contact angles of polar liquid (distilled water) droplets on the film surface. Contact angles were determined by a *Rammé-Hart 100-00* Goniometer, and the results are the average of 8 values measured at 4 different locations of the surface.

2.6- Scanning electron microscope (SEM)

The morphology of samples was obtained using a scanning electron microscope (JEOL JSM 6010). The fracture surface was coated with a thin layer of evaporated gold. The beam acceleration voltage was 20kV, secondary electrons detector were used to generate the micrograph.

2.7- Tensile testing

For the tensile tests, specimens were made according to ASTM D638. The tests were performed in quadruplicate using an TA.XT Plus Texture Analyzer - Stable Micro Systems machine with mini tensile grips at 25°C with a strain rate of 1.5mm.min⁻¹.

2.8- Differential scanning calorimetry (DSC)

Differential scanning calorimetry (DSC) was done using a TA Instruments device with a low temperature accessory. The DSC measurements were done at a heating rate of 10°C/min in a nitrogen atmosphere and in the temperature range of -20 to 500°C. The glass transition temperature (T_g) was taken at the midpoint of the stepwise specific heat increment.

3.RESULTS AND DISCUSSION

3.1- Fourier Transform Infrared (FTIR) spectroscopy

The FTIR spectra of the PLDLA-co-TMC and 50W or 100W are shown in Figure 1. The tests of each sample are performed after drying by casting method. Analyzing the infrared spectrum, the structural conformation of SF can be determined, depending on the peak location of the absorption bands of amides I, II and III. The amide I absorption arises predominantly from protein amide C=O stretching vibrations, the amide II absorption is made up of amide N-H bending vibrations and C-N stretching vibrations (60% and 40% contribution to the peak respectively); the amide III peak is complex, consisting of components from C-N stretching and N-H in plane bending from amide linkages, as well as absorptions arising from wagging vibrations from CH₂ groups from the glycine backbone and proline side-chains.¹⁹⁻²¹

Is possible to note also in Figure 1 that SF presented absorption peaks at 1641 cm⁻¹ and 1632 cm⁻¹ (amide I) and 1515 cm⁻¹ (amide II), corresponding to the SF silk II structural conformation (β-sheet). Other absorption bands were observed at 1530 cm⁻¹ (amide II) and 1237 cm⁻¹ (amide III), which are characteristic of the silk I conformation (random coil and α-helix). This indicates that silk I and silk II structures are presented simultaneously in SF.²²

After SF have been add incorporated in PLDLA-co-TMC (1:1 w/w) is interesting to note in the infrared spectra that the absorption bands of SF cannot be observed. So the disappearance of absorption bands of SF could suggest that there was a slight interaction between amide group of SF and PLDLA-co-TMC.

3.2- Scanning electron microscope (SEM)

Figure 2 shows the surface of PLDLA-co-TMC (50/50) (a), SF (b) and PLDLA-co-TMC (50/50) + 5% SF dispersed by 50W (c) and 100W (d) potency. Figure 2(b) shows that SF present a morphology similar to plates. It can be seen that these plates are mainly composed by sheet with the size apparently above than 10µm. Figure 2 (a) shows that the PLDLA-co-TMC (50/50) film presents a smooth and homogenous surface. In turn, Figures 2 (c) and 2(d) show that the addition of SF in PLDLA-co-TMC (50/50) leaves the polymer surface more irregular. I.e. apparently the polymer surface becomes more roughened. Furthermore. it shows also that the fibroin is not solubilized by PLDLA-co-TMC (50/50).

Another observation that can be done on the Figures 2(c) and 2(d) is in relation to different potency (50 to 100W) used in the preparation of polymeric film loaded with fibroin. These different potencies can interfere in

the SF dispersion on the polymeric surface. In this case in lower potency the SF showed better dispersion on the PLDLA-co-TMC (50/50) surface (Figure 2(c)) than at higher potency (Figure 2(d)). Moreover, it notes that the potency of ultrasonic tip used to disperse the SF in polymer solution destroys the plates form of SF and there is also a recoating process of SF by PLDLA-co-TMC that is more pronounced in 100W potency than 50W potency.

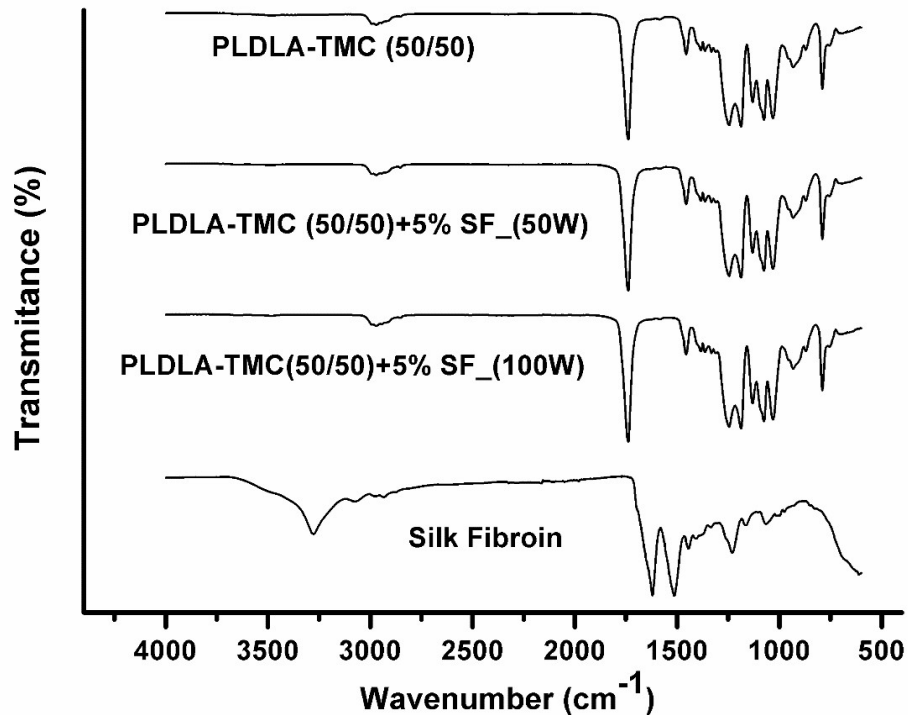


Figure 1. FTIR spectra of PLDLA-co-TMC, 50W, 100W membrane and Silk Fibroin after freeze drying. Furthermore, infrared spectra is very useful for analyzing TMC and lactide copolymers. Specifically, the peaks attributed to the presence of TMC occur at 1745 cm^{-1} (C=O) and 1247 cm^{-1} (OCO), the latter involving asymmetrical stretching, while peaks corresponding to PLDLA occur at 1757 cm^{-1} and 1185 cm^{-1} (C=O and COC, respectively).¹⁷

The contact angle (θ) measure was performed to evaluate the surface of the 50W and 100W samples. The surface properties will influence the performance of a biomaterial in a biological environment. For example, the hydrophilicity of material is an important factor for cell adhesion and growth, and improved surface hydrophilicity of materials will improve the interactions between the composites and cells for eliciting controlled cellular adhesion and maintaining differentiated phenotypic expression.²³

Silk I, the other main crystal structure of SF, is a hydrated structure and is considered to be a necessary intermediate for the preorganization or realignment of silk fibroin molecules. Figure 3 illustrates the dynamic contact angle, it is possible to show that the PLDLA-co-TMC (1:1 w/w) has a contact angle value higher than the others samples with SF (50W e 100W), this result has been caused by PLDLA-co-TMC hydrophobicity. On the other hand, the incorporation of SF increase hydrophilicity of PLDLA-co-TMC:SF decrease the contact angle values when compared to PLDLA-co-TMC, i. e. increase the hydrophilicity of system. This result shows that the potency of sonication, 50 W or 100W, have important role in the dispersion of SF powder changing the contact angle of approximately 10° and 6° for the potency of 50W and 100W, respectively. This minor decrease on the contact angle value for the sample prepared to 100W potency in relation to 50W potency, compared to PLDLA-

co-TMC polymer, is according to images seen in Figure 2. In this case two possibilities can be considered (i) using 100W of potency there was a covered of SF by the polymer more effective than 50W of potency; (ii) silk I structure was partially transformed to silk II structure (more hydrophobic) after sonication process with 100W of potency. Thus, the reduction of contact angle value in the sample prepared to 50W potency is due the presence of more hydrophilic groups (silk I) on the surface of PLDLA-co-TMC polymer. So, the reduction of θ value shows that SF dispersed also on the membrane surface would be an important feature that an effective bandage for skin burn must present. Once allows fast contact between SF and skin damaged area. This way the healing skin process would be accelerated.

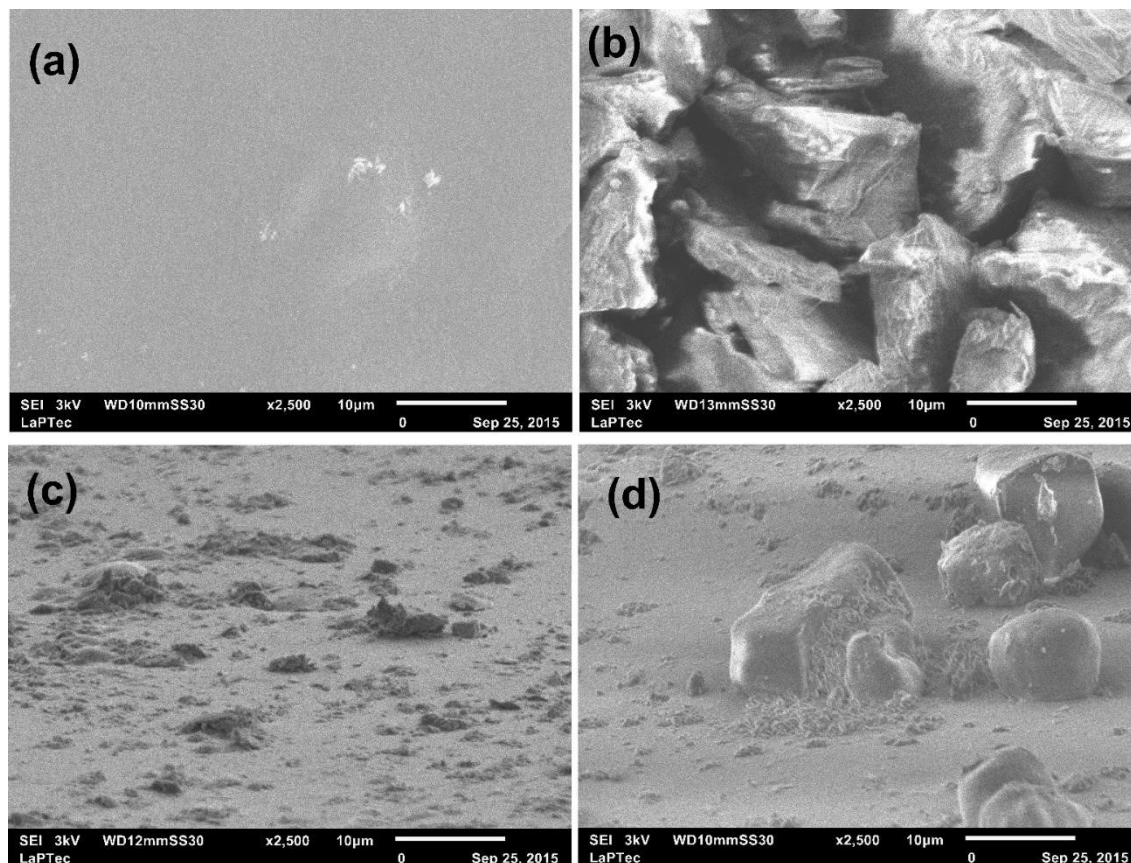


Figure 2. SEM Micrographs of sample PLDLA-co-TMC (a), Silk Fibroin (b), 50W (c) and 100W (d).

3.4- Swelling test

Figure 4 illustrates the weight change versus immersion time of samples in PBS solution at 37°C, according to the sonication potency. According to Figure 4 the PLDLA-co-TMC (50/50) presents a slight weight gain over the test, increasing its initial weight around 3.2%. This result shows the hydrophobic behavior of this polymer, corroborating the contact angle test. On the other hand, the samples with 5% SF shows a different behavior compared to PLDLA-co-TMC. Initially both samples of prepared with 50W and 100W of potency showed a liquid absorption rate faster than the PLDLA-co-TMC. However, after this period the liquid absorption behavior was changed. The sample 50W showed a smooth weight gain, reaching about 8.4% of the initial weight. In turn, sample 100W showed a sharp weight gain, reaching a about 17% of initial weight. Therefore, the difference in the final weight gain of 50 and 100W samples can be explained by adsorption and absorption phenomena and more degradation of fibroin I (hydrophilic) than fibroin II (less hydrophilic).

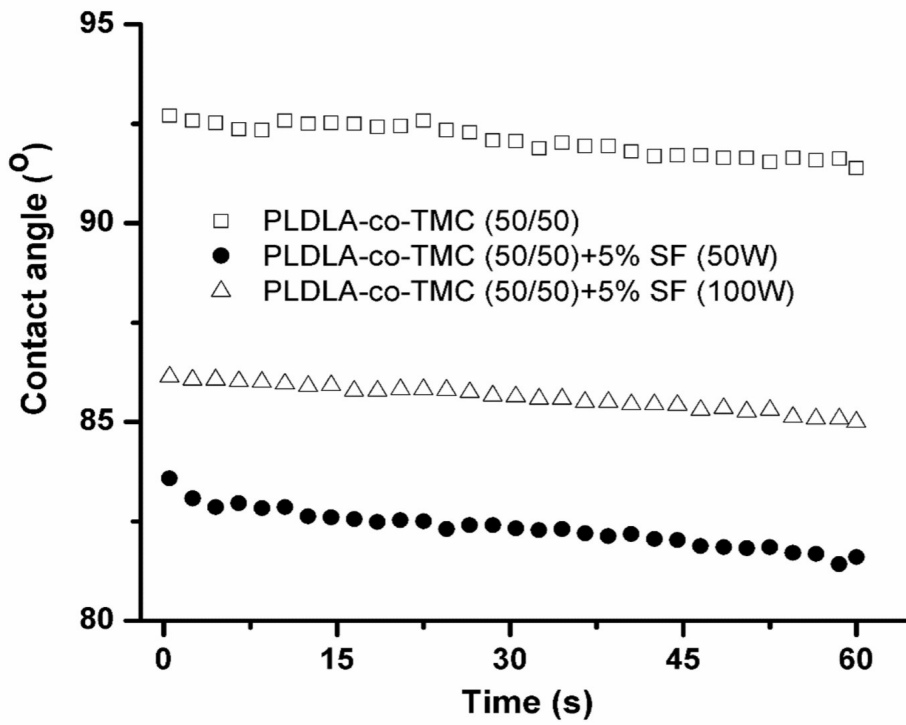


Figure 3. Contact angle versus time

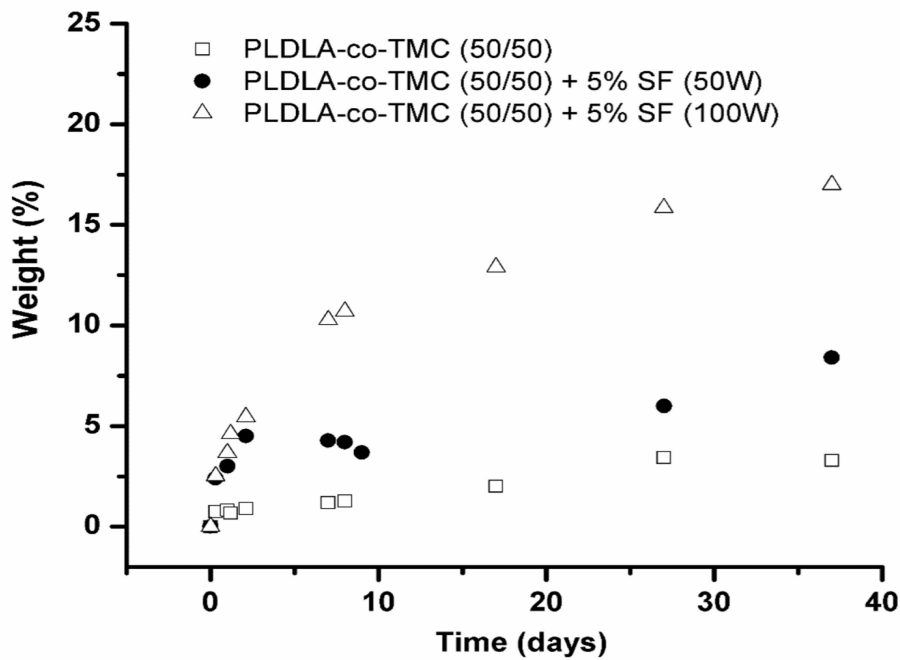


Figure 4. Weight (%) versus time (days).

3.5- Tensile testing

The curves in Figure 5 shows that PLDLA-co-TMC (50/50) polymer presents an elastomeric behavior as well as after addition of SF in this polymer. This is due to the presence of trimethylene carbonate (TMC) in the material structure. Until 2MPa tension the curves are similar, but from 2MPa there are a difference between the curves as a function of the sample submitted to stress. It is possible to note also that the presence of SF increases the deformation of PLDLA-co-TMC (50/50). This is an important characteristic that wound dressing need to have because it indicates their ability to conform to damaged skin, i.e. it is necessary that the wound dressing shows good flexibility. Figures 6 and 7 shows the Young's Modulus (MPa) and elongation at break (%), respectively.

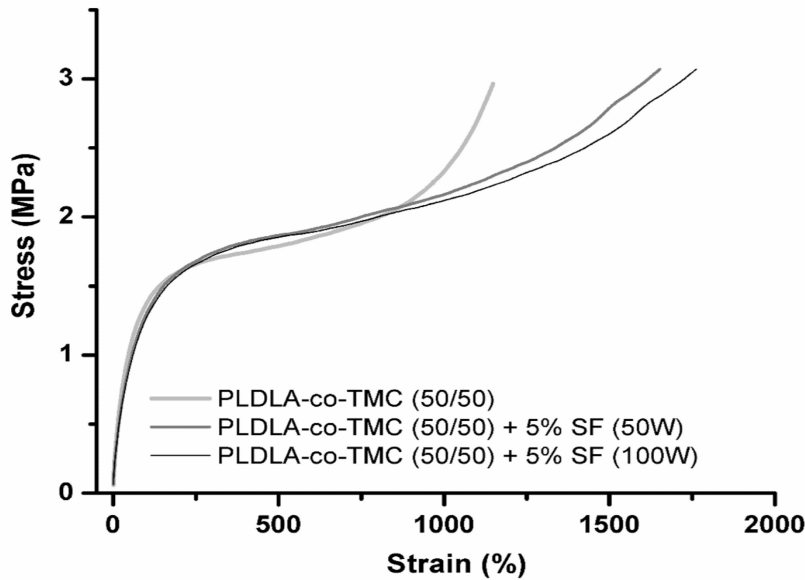


Figure 5. Stress (MPa) Versus Strain (%) of of sample PLDLA-co-TMC, 50W and 100W.

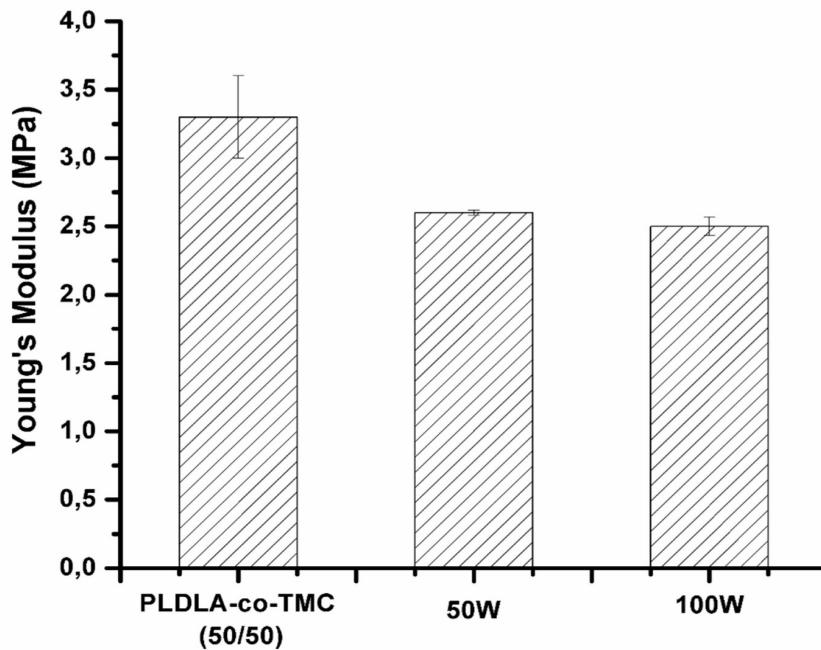


Figure 6. Young's Modulus of sample PLDLA-co-TMC, 50W and 100W

and increases their elongation at break values. So this behavior could be explained because the SF would act as a lubricant that would facilitate the slipping between polymer chains during the mechanical testing. It is possible to verify that the SF exhibits a lubricant effect analyzing the DSC thermogram showed in Figure 8. i.e. after SF be added in the PLDLA-co-TMC (50/50) practically there was not change on their glass temperature (T_g) when compared to PLDLA-co-TMC (50/50) indicating that SF acts as lubricant and not as plasticizer in the PLDLA-co-TMC (50/50).

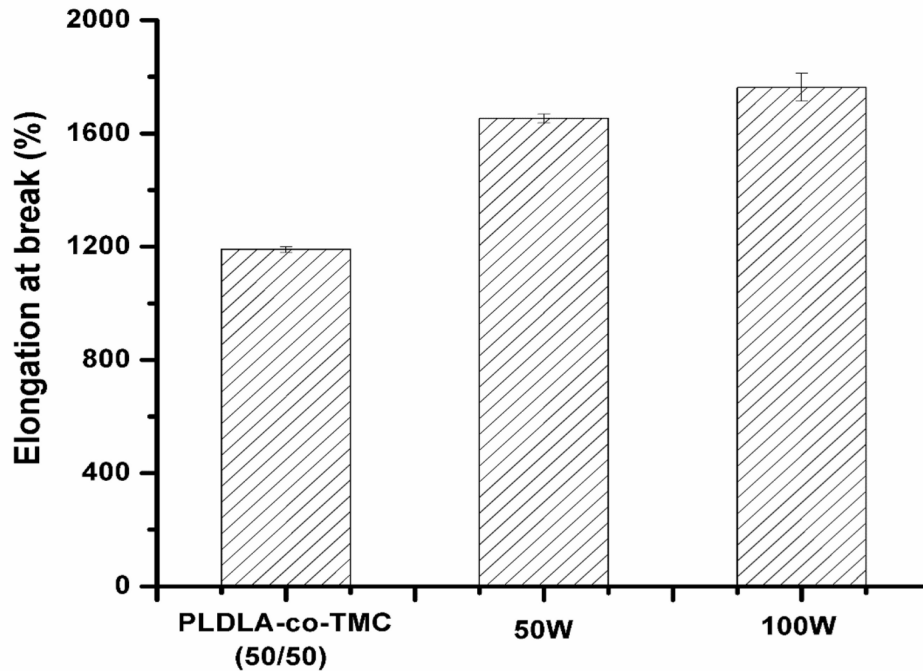


Figure 7. Elongation at break (%) of sample PLDLA-co-TMC, 50W and 100W

Moreover, the different potencies of sonication used to mixture SF in the PLDLA-co-TMC (50/50) did not influence significantly the mechanical property of composite obtained, despite of structural difference that have been seen in the SEM micrographs showed in Figure 2. It is possible to note that the Young's Modulus of PLDLA-co-TMC (50/50)+5% SF (100W) is slight smaller than PLDLA-co-TMC (50/50)+5% SF (50W). Besides that, is possible to note also the elongation at break of PLDLA-co-TMC (50/50)+5% SF (100W) is slight bigger than slight PLDLA-co-TMC (50/50)+5% SF (50W). Therefore, the presence of biggest SF aggregates reduces Young's Modulus values and increases elongation at break values when compared with small SF aggregates, i.e. the big SF aggregates has lubricant effect slightly better than small SF aggregates.

3.6- Differential scanning calorimetry (DSC)

Figure 8 shows the DSC thermogram for SF. There are two broad endotherms peaks, one at low temperature (below 150°C), due to loss of moisture, another at high temperature (endo peak at 291°C), attributed to thermal degradation of silk. Moreover, SF did not show any trace of the thermal transitions occurring at around 200°C . These, in fact, are attributed to the heat-induced random coil \rightarrow β -sheet conformational transition of the fibroin chains. Their absence may indicate that the crystallization process has already achieved its completion during the coagulation and drying phases. The decomposition behavior of silk is influenced by the intrinsic morphological and physical properties of the sample, the degree of molecular orientation being one of the most important parameters. Well oriented SF fibers usually exhibit a decomposition peak located at above 300°C . Silk materials, randomly distributed, with β -sheet crystalline structure usually decompose in the 290 - 295°C temperature range, while decomposition of amorphous SF occurs at lower temperature ($< 290^{\circ}\text{C}$). Therefore, according to thermal degradation temperature (Figure 8) the randomly distributed SF was used in this work.²⁴ The tests of each sample are performed after drying by casting method.

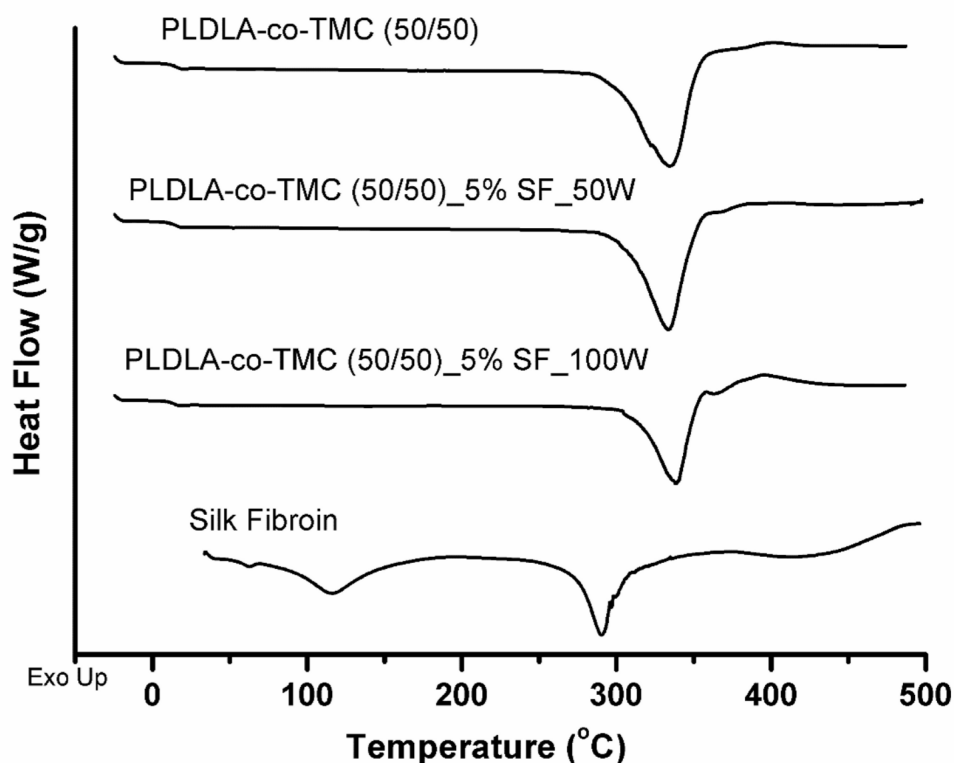


Figure 8. DSC curves of sample PLDLA-co-TMC 50W and 100W and Silk Fibroin after drying

Figure 8 shows also the DSC thermogram for PLDLA-co-TMC (50/50), PLDLA-co-TMC (50/50) + 5% SF (50W) and PLDLA-co-TMC (50/50) + 5% SF (100W). After SF be added in the PLDLA-co-TMC (50/50) there was no change in the profile of curves. However, the glass transition temperature (T_g) of PLDLA-co-TMC (50/50) slightly decreases with addition SF as shown in Table 1.

Table 1. Glass transition temperature (T_g) of PLDLA-co-TMC (50/50), PLDLA-co-TMC (50/50) + 5% SF (50W) and PLDLA-co-TMC (50/50) + 5% SF (100W).

Sample	T_g (°C)
PLDLA-co-TMC (50/50)	17.0
PLDLA-co-TMC (50/50) + 5% SF (50W)	16.1
PLDLA-co-TMC (50/50) + 5% SF (100W)	14.5

According to the T_g values showed in Table 1 is not possible to affirm that SF behaves as plasticizer because this temperature variation is very small and little significant. However, there are two possible effects that SF can provide: a lubricant effect and a decrease in the intensity between polymer chains.

Lubricity and gel theories have been extensively used to explain the effects of plasticizers on polymeric structures. Lubricity theory proposes that the plasticizer can exert a lubricant effect which leads to increased chain mobility as the distance between polymer chains increases thus leading to decreased polymer– polymer interac-

tions. On the other hand, the gel theory suggests that the plasticizer contributes to lower polymer–polymer interactions (hydrogen bonds, van der Waals or ionic forces, etc.) which has a positive effect on the overall chain mobility. These phenomena could explain the observed decrease in T_g values as SF is added.²⁵

Moreover, the PLDLA-co-TMC (50/50) + 5% SF (100W) sample shows more reduction on T_g value than PLDLA-co-TMC (50/50) + 5% SF (50W). It happens because the highest potency used to disperse SF on the PLDLA-co-TMC (50/50) generates big SF aggregates with lubricant effect slightly better than small SF aggregates.

CONCLUSIONS

Elongation at break of PLDLA-co-TMC (50/50) increased after SF have been added. So this behavior could be explained because the SF would act as a lubricant that would facilitate the slipping between polymer chains during the mechanical testing. In addition, the potency used to disperse the SF also influences the elongation at break of PLDLA-co-TMC (50/50). PLDLA-co-TMC (50/50) presents a slight weight gain over the test. It shows the hydrophobic characteristic of this polymer. On the other hand, after addition of SF in the PLDLA-co-TMC (50/50) there was an increase of liquid weight gain showing that the SF is hydrophilic. The thermal degradation temperature observed in DSC thermogram confirmed the presence of SF, randomly distributed, used in this work. Moreover, there was a decrease of T_g value after SF has been added in PLDLA-co-TMC (50/50). So it could be explained because the SF would act as a lubricant that would facilitate the slipping between polymer chains during the mechanical testing. SEM images shows that the best dispersion of SF on the PLDLA-co-TMC (50/50) surface is achieved using low potency. The incorporation of SF on the PLDLA-co-TMC (50/50) reduces the contact angle values compared to PLDLA-co-TMC (50/50). I. e. the PLDLA-co-TMC (50/50) surface become less hydrophobic. This result showed that the potency of sonication has important role on the dispersion of SF, causing a reduction in the contact angle compared to PLDLA-co-TMC (50/50). Despite the FTIR results do not show clearly the incorporation of fibroin in PLDLA-co-TMC (50/50) films, this was confirmed by SEM micrographs.

ACKNOWLEDGMENTS

The authors would like to thank the FAPESP, CNPq and CAPES by financial support. Furthermore, we would like to thank the Laboratory of Technological Plasmas from Universidade Estadual Paulista (UNESP) Campus Sorocaba-SP by the SEM images and contact angle measurement.

REFERENCES

- Altman, G. H.; Diaz, F.; Jakuba, C.; Calabro, T.; Horan, R. L.; Chen, J.; Lu, H.; Richmond J.; Kaplan, D. L. *Biomaterials*, 2003, 24, 401-416.
- Santin, M.; Motta, A.; Freddi, G.; Cannas, M. *J. Biomed. Mater. Res.*, 1999, 9, 382-389.
- Li, M.; Lu, S.; Wu, Z.; Tan, K.; Minoura, N.; Kuga, S. *Int. J. Biol. Macromol.*, 2002, 30, 89-94.
- Li, M. Z.; Ogiso, M.; Minoura, N. *Biomaterials*, 2003, 24, 357-365.
- Meinel, L.; Hofmann, S.; Karageorgiou, V.; Kirker-Head, C.; McCool, J.; Gronowicz, G.; Zichner, L.; Langer, R.; Vunjak-Novakovic, G.; Kaplan, D. L. *Biomaterials*, 2005, 26, 147-155.
- Badami, A. S.; Kreke, M. R.; Thompson, M. S.; Riffle, J. S.; & Goldstein, A. S. *Biomaterials*, 2006, 27, 596-606.
- Liang, D.; Hsiao, B. S.; Chu, B. *Adv. Drug Deliver. Rev.*, 2007, 59, 1392-1412.
- Lovett, M.; Eng, G.; Kluge, J. A.; Cannizzaro, C.; Vunjak-Novakovic, G.; Kaplan, D. L.
- Organogenesis*, 2010, 6, 217-224.
- Leal-Egana, A.; Scheibel, T. *Biotechnol. Appl. Bioc.*, 2010, 55,155-167.
- Qu, Y.; Yang, Y.; Li, J.; Chen, Z.; Li, J.; Tang, K.; Man, Y. *J. Biomater. Appl.*, 2011, 26, 311–325.
- Zhang, K.; Wang, H.; Huang, C.; Su, Y.; Mo, X.; Ikada, Y. *J. Biomed. Mater. Res. Part A*, 2009, 93, 984-993.
- Vachiraroj, N.; Ratanavaraporn, J.; Damrongsakkul, S.; Pichyangkura, R.; Banaprasert, T.; Kanokpanont, S. *Int. J. Biol. Macromol.*, 2009, 45, 470-477.
- Elia, R.; Newhide, D. R.; Pedevillano, P. D.; Reiss, G. R.; Firpo, M. A.; Hsu, E. W.; Kaplan, D. L.; Prestwich, G. D.; Peattie, R. A. *J. Biomater. Appl.*, 2013, 27,749-762.
- Kundu, J.; Poole-Warren, L. A.; Martens, P.; Kundu, S. C. *Acta Biomaterialia*, 2012, 8, 1720-1729.
- Rasal, R. M.; Janorkar, A. V.; Hirt, D. E. *Prog. Polym. Sci.*, 2010, 35, 338-356.
- Zhang, Z.; Kuijter, R.; Bulstrab, S. K.; Grijpma, D. W.; Feijen, J. *Biomaterials*, 2006, 27, 1741-1748.
- Motta, C. A.; Duek, E. A. R. *Mater. Res.*, 2014, 17, 619-626.
- Rockwood, D. N.; Preda, R. C.; Yücel, T.; Wang, X.; Lovett, M. L.; Kaplan, D. L. *Nature Protocols*, 2011, 6, 1612-1631.

21. Sionkowska, A.; Lewandowska, K.; Michalska, M.; Walczak, M. *J. Mol. Liq.*, 2016, 215, 323-327.
22. Wang, J.; Yang, Q.; Cheng, N.; Tao, X.; Zhang, Z.; Sun, X.; Zhang, Q. *Mater. Sci. Eng. C: Materials for Biological Applications*, 2016, 61, 705–711.
23. Bhardwaj, N.; Rajkhowa, R.; Wang, X.; Devi, D. *Int. J. Biol. Macromol.*, 2015, 81, 31-40.
24. Moraes, M. A.; Nogueira, G. M.; Weska, R. F.; Beppu, M. M. *Polymers*, 2010, 2, 719-727.
25. Zhu, H.; Liu, N.; Feng, X.; Chen, J. *Mater. Sci. Eng. C: Materials for Biological Applications*, 2012, 32, 822-829.
26. Freddi, G.; Pessina, G.; Tsukada, M. *Int. J. Biol. Macromol.*, 1999, 24, 251-263.
27. Ferri, J. M.; Garcia-Garcia, D.; Sánchez-Nacher, L.; Fenollar, O.; Balart, R. *Carbohydr. Polym.*, 2016, 147, 60-68.

SIFT DESK

Deerpark Dr, #75, Fullerton, CA, 92831, United States.

E-mail:

helpdesk@siftdesk.org

Visit us on the web at:

www.siftdesk.org